Catalysis Today 170 (2011) 134–140

Contents lists available at ScienceDirect

Catalysis Today

journal homepage: www.elsevier.com/locate/cattod

Platinum-rare earth intermetallic alloys as anode electrocatalysts for borohydride oxidation

D.M.F. Santos[a,*], P.G. Saturnino[a], D. Macciò[b], A. Saccone[b], C.A.C. Sequeira[a]

[a] Materials Electrochemistry Group, Institute of Materials and Surfaces Science and Engineering, Instituto Superior Técnico, TU Lisbon, 1049-001 Lisboa, Portugal
[b] Università degli Studi di Genova, Dipartimento di Chimica e Chimica Industriale (DCCI), via Dodecaneso 31, I-16146 Genova, Italy

ARTICLE INFO

Article history:
Available online 1 June 2011

Keywords:
Sodium borohydride
Oxidation
Platinum-rare earth intermetallics
Cyclic voltammetry
Chronopotentiometry
Direct borohydride fuel cells

ABSTRACT

Sodium borohydride ($NaBH_4$) is being actively investigated as an anodic fuel for direct borohydride fuel cells. Platinum (Pt) displays a rather good borohydride (BH_4^-) oxidation activity but its catalytic effect towards the BH_4^- hydrolysis leads to an overall number of exchanged electrons in the oxidation process, n, between 2 and 4. The doping of Pt with rare earth (RE) elements may decrease or increase the BH_4^- hydrolysis, thereby increasing or decreasing the n value. Among other factors, these changes will depend on the composition of the alloying elements as well as on the applied anodic potential range. In this paper, Pt and three Pt–RE intermetallic alloy (Pt–Ho, Pt–Sm, and Pt–Ce) electrodes are studied by cyclic voltammetry (CV) and chronopotentiometry (CP) in the temperature range 25–55 °C. Modelling of CV and CP data indicate that these Pt–RE electrodes do not show enhanced performance for the BH_4^- oxidation in comparison to the single Pt electrocatalyst. Of the Pt alloys, the Pt–Ho shows the highest catalytic activity for the BH_4^- oxidation reaction and the Pt–Ce the worst. Relevant kinetic parameters (n, α, k_s) are also estimated.

1. Introduction

Sodium borohydride ($NaBH_4$) is receiving increasing attention during the last decade regarding its possible application in energy systems [1–4]. $NaBH_4$ shows interesting options for electrochemical power generation for having the dual possibility of generating hydrogen on demand [5,6] or being directly oxidised in a direct borohydride fuel cell (DBFC) [7–11]. $NaBH_4$ has the advantage of having a high volumetric (7314 Wh dm^{-3}), as well as gravimetric (7100 Wh kg^{-1}), energy density [12]. Moreover, alkaline $NaBH_4$ solutions are safe to transport and tetrahydroxyborate ($B(OH)_4^-$), the final product of borohydride (BH_4^-) electrooxidation, is environmentally safe. For these motives, the DBFC technology is being actively investigated by many research groups [13–19], with electrical performances as high as 290 mW cm^{-2} being reported [8].

The mechanisms recently proposed to explain the BH_4^- direct/indirect oxidation are still not clearly established. However, the following explanation may serve as a basis to address the question. In highly alkaline conditions, BH_4^- may undergo an 8-electron oxidation described by Eq. (1).

$$BH_4^- + 8OH^- \rightarrow B(OH)_4^- + 4H_2O + 8e^- \quad (1)$$

However, for pH < 12 or in the presence of certain electrocatalysts, BH_4^- is susceptible to catalytic hydrolysis on the electrode surface [20], which generates hydroxyborohydride (BH_3OH^-) and H_2 according to Eq. (2) [21–26].

$$BH_4^- + H_2O \rightarrow BH_3OH^- + H_2 \quad (2)$$

In fact, the BH_4^- oxidation reaction and the BH_4^- hydrolysis reaction are always present, meaning that both reactions can either be complete, or compete together [27–30]. Therefore, the BH_3OH^- intermediate formed in Eq. (2) may be fully oxidised according to Eq. (3), yielding 6 electrons without any H_2 release. In this case, the anodic wave for the oxidation of the BH_3OH^- (Eq. (3)) appears at a potential about 0.5 V more negative than that of BH_4^- direct oxidation (Eq. (1)) [31–33].

$$BH_3OH^- + 6OH^- \rightarrow B(OH)_4^- + 3H_2O + 6e^- \quad (3)$$

Alternatively, BH_3OH^- may undergo stepwise oxidations [34] involving only 3 electrons in total with the simultaneous generation of H_2, as shown in Eq. (4).

$$BH_3OH^- + 3OH^- \rightarrow B(OH)_4^- + 3/2H_2 + 3e^- \quad (4)$$

Part of the generated H_2 remains on the electrode surface and then may be oxidised through the reaction shown in Eq. (5).

$$1/2H_2 + OH^- \rightarrow H_2O + e^- \quad (5)$$

* Corresponding author. Tel.: +351 218417765; fax: +351 218417765.
E-mail address: diogosantos@ist.utl.pt (D.M.F. Santos).

0920-5861/$ – see front matter © 2011 Elsevier B.V. All rights reserved.
doi:10.1016/j.cattod.2011.03.037

The indirect oxidation reaction of BH_4^- via the oxidation of the BH_3OH^- intermediate involving H_2 evolution and its subsequent oxidation can then be described by Eq. (6), which corresponds to the addition of Eqs. (2), (4) and (5).

$$BH_4^- + 4OH^- \rightarrow B(OH)_4^- + 2H_2 + 4e^- \quad (6)$$

This process (Eq. (6)) is typically observed in metals like platinum, palladium, or nickel. These metals are known to be able to oxidise BH_4^- at low overpotentials [35], but have the drawback of being simultaneously catalysts for the BH_4^- hydrolysis [27,28,36–40]. For this reason, many authors have reported that the typical number of exchanged electrons, n, ranges from 2 to 4 for platinum (Pt) electrocatalysts [30,35,41]. Therefore it is imperative to develop new Pt alloys that can still oxidise the BH_4^- ion at low overpotentials but with increased n values [42].

Reported experience with rare earth (RE) alloys [43–49], and specifically Pt–RE alloys [50], have shown the superior electrocatalytic activity of the Pt–RE alloys for the hydrogen evolution reaction (HER) compared to Pt alone [50]. Moreover, recent studies have also demonstrated that Pt–RE alloy electrodes present higher catalytic activity towards the methanol [51] and ethanol [52–54] electrooxidation, in comparison to a single Pt electrocatalyst.

Technological applications of Pt–RE alloys, namely in the fields of magnetic materials [55,56], catalysis [57], and high temperature oxidising environments [58], can be justified independently of their high cost. For example, due to the growing interest of fuel cells, where they are used, e.g., for water gas-reforming [59], they may be adequate as anodes for DBFCs or for the heterogeneous hydrolysis of BH_4^-, the resulting H_2 being used in $NaBH_4$–PEMFC systems, as reported by Demirci and Miele [60].

The increased catalytic activity of Pt–RE electrodes may be justified on the basis of improved three-dimensional hydridic factors of composite electrocatalysts as first pointed out by Vračar and Conway [61,62]. The Brewer-Engel theory [63], more recently refined by Jaksic et al. [64–66], allows us to consider that Pt-RE/BH_4^- interfaces can be interesting systems to the PEMFC or to the DBFC. In this context, the relative favourability of each type of fuel cell should depend on the nature and composition of the alloying elements (Y, La, Ce, Sm, Dy, Ho, Er, ...), as well as on the applied electrode potential range.

So, the DBFC's efficiency is strongly dependent on the anode electrocatalyst in whose surface the BH_4^- oxidation occurs. Gold (Au) has been reported as being able of achieving the complete 8-electron oxidation of the BH_4^- ion [20,67–69]. However, the oxidation kinetics in the Au surface is so slow that it loses importance for use in the DBFC's anode. In contrast, the kinetics of the BH_4^- oxidation reaction in Pt is much faster [26] but Pt does not suppress the competing hydrolysis of BH_4^-, which is also a prerequisite for DBFCs. It has been suggested by several authors [40,70–73] that the most suitable metal to suppress the BH_4^- hydrolysis should be silver (Ag). Therefore, it is clear that much work still has to be done. In fact, higher fuel efficiency, adequate safety, system design, and durable membrane electrode assemblies (MEAs), require a deeper understanding of the BH_4^- oxidation at the DBFC anode [11].

To increase the current efficiency of the DBFC it is expected that new Pt alloy electrocatalysts may enhance the direct reaction pathway (Eq. (1)) or, at least, to favour the process described by Eq. (3) (obviously with a small theoretical efficiency loss). For the present work, the BH_4^- oxidation at Pt and three Pt–RE intermetallic alloy electrodes (Pt–Ho, Pt–Sm, and Pt–Ce) is studied by cyclic voltammetry (CV) and chronopotentiometry (CP) experiments.

CV is a very popular electrochemical method that is particularly powerful for initial studies of a new system. Many experiments can be carried out within a few minutes. Moreover, the data are presented in a form that allows rapid, qualitative interpretation without need of detailed calculation. Therefore, the insight gained from one experiment may immediately be used in the design of the next. Of course, the voltammograms are also capable of quantitative analyses and lead to relevant kinetic data, namely for the BH_4^- electrooxidation [16,20,37,39,68,74–76]. In this context, certain kinetic parameters, such as the anodic charge transfer coefficients, α, for the BH_4^- oxidation on the Pt–RE catalysts are calculated in the present paper by using CV.

Further insights in the complex electrochemical behaviour of BH_4^- are obtained by employing CP measurements. By analogy with the constant current operation of a DBFC, CP can be used for studying the BH_4^- electrooxidation [28,37,67,70,71,77,78], providing relevant information regarding the Pt–RE/BH_4^- system. In this situation, the current applied to a cell is stepped from an initial value ($i = 0$) where the electrode potential for the $B(OH)_4^-/BH_4^-$ couple is at equilibrium ($E = E_e$), to a final value where the electrode reaction of interest takes place. The potential–time response is then recorded and analysed. In practice, the BH_4^- species near the electrode are quickly oxidised and the diffusion layer grows. The $B(OH)_4^-/BH_4^-$ ratio at the electrode surface increases and the potential swings positive. Eventually, diffusion can no longer supply enough BH_4^- to provide the required current and the potential heads toward $+\infty$. The time required for this potential swing is called the transition time, τ. Here, detailed measurements of these τ values, at different experimental conditions, allowed a thorough characterisation of the BH_4^- oxidation on the Pt and Pt–RE electrodes, complemented by the determination of the total number of exchanged electrons, n and the heterogeneous standard rate constant, k_s.

2. Experimental

2.1. Preparation of the Pt–RE electrocatalysts

Binary alloys with equiatomic compositions were prepared by weighing stoichiometric amounts of small pieces of the two elements, which were then sealed in tantalum crucibles under argon atmosphere. The crucibles were subsequently induction heated under an inert gas flux (argon), repeatedly shaking the crucibles to obtain homogenisation. Alloys with uniform composition are generally obtained by this method without any contamination by the crucible material.

Prior to the electrochemical tests, the alloys were analysed by SEM (Scanning Electron Microscopy) and EDX (Energy Dispersive X-ray analysis) to characterise their morphology and composition.

2.2. Electrochemical measurements

Electrode reaction rates and other relevant electrochemical parameters to be calculated are extensive quantities and have to be referred to the unit area of the electrode/BH_4^- solution interface. The real surface area, A_s or the electrochemical surface area, of the Pt and Pt–RE alloy electrodes that were used as working electrodes was determined by linear sweep voltammetry, as described by Trasatti and Petrii [79]. Basically, voltammetric curves are recorded in a narrow potential range at different potential scan rates. The current in the middle of the potential range is then plotted as a function of the scan rate. Under the assumption that double layer charging is the only process, a straight line outcomes, whose slope gives the differential capacitance of the interface. The capacitance thus obtained is then compared to a reference value so that A_s is calculated. Since the accuracy of A_s impacts the qualitative and quantitative results, these tests approached as much as possible the experimental situation to which the calculated areas are to be applied [79]. In this way, A_s values of 3.0, 0.74, 0.72, and 0.61 cm^2 were calculated for the Pt, Pt–Ce, Pt–Ho, and Pt–Sm electrodes, respectively. These A_s

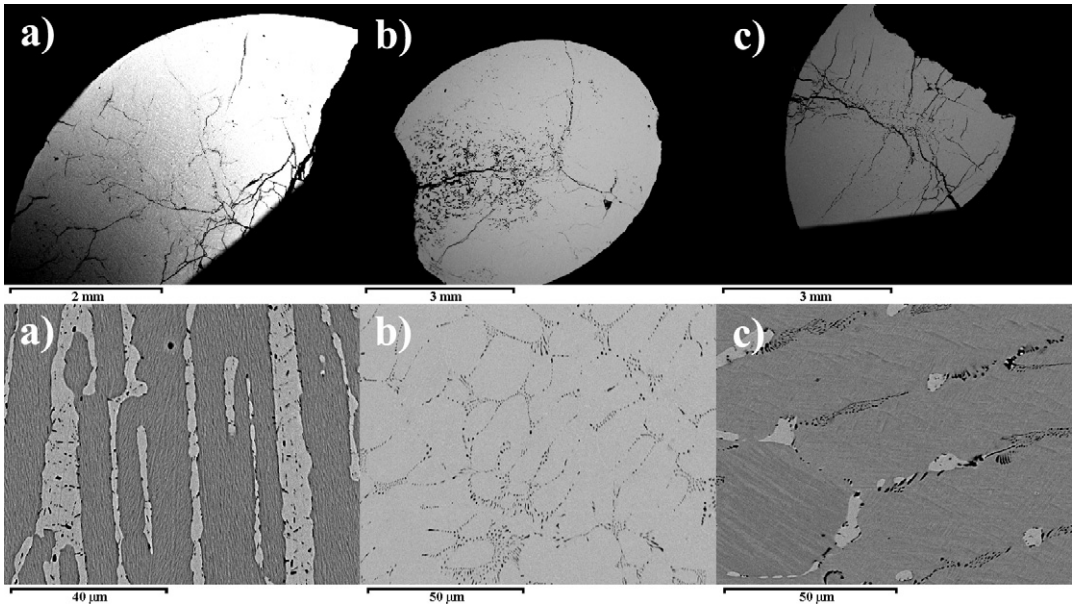

Fig. 1. SEM microphotographs of the prepared Pt–RE alloys: (a) Pt–Sm; (b) Pt–Ho; (c) Pt–Ce.

values were used throughout the present work to determine the current densities.

The electrochemical experiments were performed using a conventional three-electrode arrangement composed of one of these Pt-based working electrodes, a Johnson Matthey Pt mesh counter electrode ($A \approx 100\,cm^2$), and a Metrohm 6.0701.100 saturated calomel reference electrode (SCE). All electrode potentials are presented vs. SCE. Prior to the electrochemical testing, the surface of the working electrodes was polished with a Buehler polishing cloth, using a diamond polishing compound Metadi II (Buehler, USA). The electrodes were then cleaned by ultrasonication (Bandelin Sonorex Super RK 106) in acetone, followed by rinsing with deionised water. The test solutions were composed of 0.03 $NaBH_4$ (Merck, 98 wt.%) in 2 M NaOH (Normapur, 99 wt.%) supporting electrolyte. To prevent possible loss of BH_4^-, by hydrolysis during storage, the solutions were prepared immediately before the measurements. The electrochemical cell, whose effective cell volume was 125 cm^3, had a thermostatic water jacket for controlling the solution temperature in the range 25–55 °C (±0.1 °C) set by a recirculating water bath (Ultraterm 6000383 P-Selecta). A PAR 273A computer-controlled potentiostat (Princeton Applied Research Inc.) and the associated PowerSUITE package were employed for total control of the experiments and data acquisition.

For the four tested Pt-based electrodes (Pt, Pt–Ho, Pt–Sm, Pt–Ce), cyclic voltammograms were obtained by scanning the working electrode potential from the open circuit potential ($E_i \approx -1.0$ V vs. SCE) to a potential of about 0.5 V vs. SCE, at scan rates ranging from 2×10^{-4} V s^{-1} to 20 V s^{-1}. Regarding the chronopotentiometric measurements, the transient potentials were recorded following a stepwise change in the cell current from zero (no BH_4^- oxidation) to a value where BH_4^- oxidation was sufficiently fast so that the BH_4^- concentration at the electrode surface was essentially zero. This implied the application of current densities, *j*, ranging from 5 to 100 mA cm^{-2}, leading to chronopotentiograms with transition times varying between 0.1 s and 15 s.

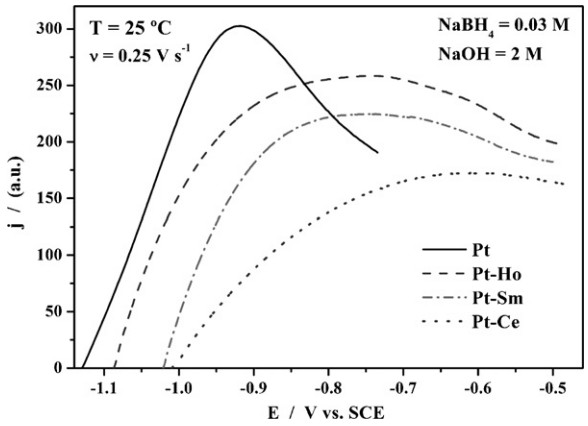

Fig. 2. Typical shape of the BH_4^- oxidation peaks obtained in the voltammograms with Pt and Pt–RE alloys, at a potential scan rate of 0.25 V s^{-1}, and at 25 °C.

3. Results and discussion

3.1. Characterisation of the Pt–RE electrocatalysts

The Pt–RE alloys were characterised by SEM and EDX in order to investigate microstructure and to measure phase compositions [50]. Fig. 1 shows the SEM microphotographs of the alloys.

The EDX measured overall composition of the two-phase Pt–Sm sample (Fig. 1a) is 50.8 at.% Pt. The grey phase is PtSm (50.2 at.% Pt), whereas the white phase at the grain boundaries is Pt_4Sm_3 (57.1 at.% Pt).

Analysis of the Pt–Ho alloy, with measured overall composition of 49.8 at.% Pt revealed an almost single phase sample (Fig. 1b). The measured average composition of the phase is 50.8 at.% Pt; small amounts of a second phase (not measured) were found at the grain boundaries.

The Pt–Ce alloy (measured overall composition 49.4 at.% Pt) shows two phases: the grey phase is PtCe (50.5 at.% Pt) and the white phase at the grain boundaries Pt_4Ce_3 (56.8 at.% Pt).

3.2. Cyclic voltammetry measurements

A typical shape of the BH_4^- electrooxidation peaks observed in the cyclic voltammograms obtained with the Pt and with the three Pt–RE alloy electrodes, in natural diffusion conditions, can be seen in Fig. 2.

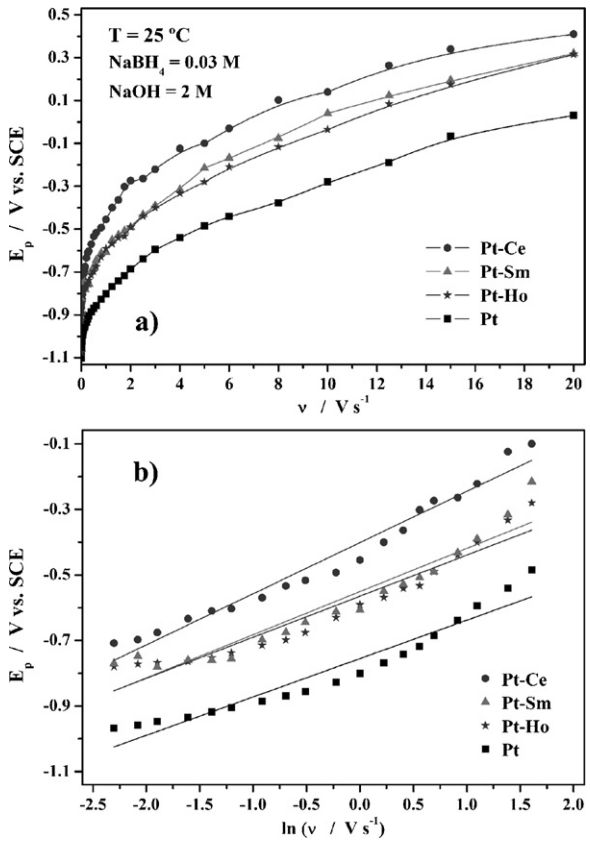

Fig. 3. (a) E_p vs. ν and (b) E_p vs. ln ν plots for the four tested electrode materials, at 25 °C.

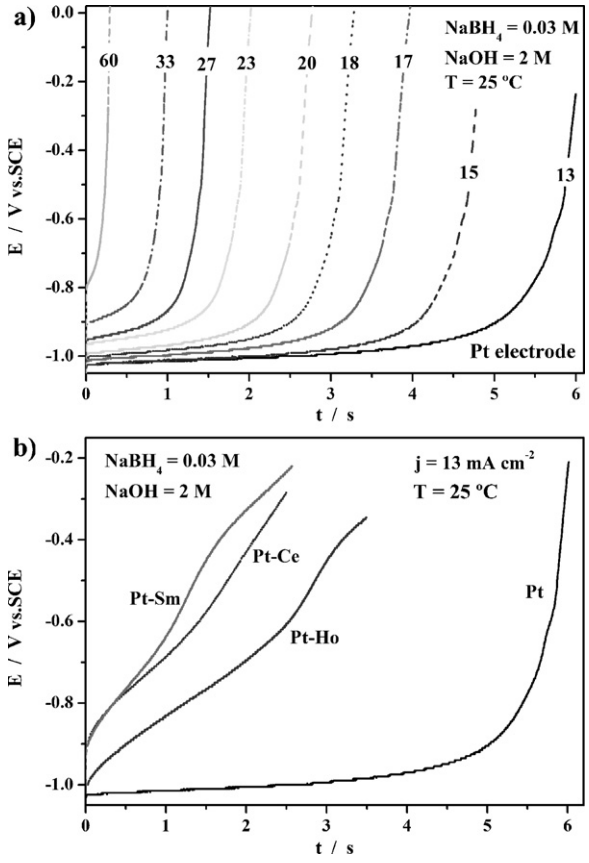

Fig. 4. (a) Effect of applied j (in mA cm^{-2}) on the chronopotentiograms for the oxidation of 0.03 M $NaBH_4$ in 2 M NaOH solution on a single Pt electrode at 25 °C. (b) Chronopotentiograms obtained with a j value of 13 mA cm^{-2}, at 25 °C, for the oxidation of 0.03 M $NaBH_4$ in 2 M NaOH solution with the four different Pt-based electrode materials.

The current density, j, axis in Fig. 2 is shown in arbitrary units (a.u.) in order to allow a better comparison between the four electrode materials. By using a.u. it is possible to compare directly the four curves in terms of their oxidation peak sharpness/broadness and its corresponding potential value. The Pt electrode voltammogram is quite similar to the current–potential responses described in the open literature [37], but those for the Pt-based alloys have a much different behaviour. It can be clearly seen that only Pt shows a sharp peak while the three alloys present a broad oxidation shoulder. Moreover, the oxidation peak for the Pt electrode occurs at very low overpotentials (η = 0.2 V), indicating superior kinetics for the BH_4^- oxidation. In contrast, the overpotentials at the point of maximum shoulder current are much higher for the Pt–RE alloys, particularly for the Pt–Ce alloy (η = 0.4 V).

E_p - ν curves depicted in Fig. 3a reveal that the peak potential, observed at the maximum j value, is due to the oxidation of an electroactive species in solution, probably BH_4^-, as suggested by Gyenge [37]. As expected for slow electron transfer irreversible processes, there is a marked shift of the oxidation peak potential, E_p, with the potential scan rate, ν (Fig. 3a).

Therefore, assuming that the peak corresponds to a single-step irreversible oxidation [37], i.e. a pure electrochemical (E) step, being the effect of BH_4^- hydrolysis practically irrelevant for the used potential domain, Eq. (7) applies [37,68,80]

$$E_p = E^0 + \left\{\frac{RT}{[(1-\alpha)n_a F]}\right\}\left\{0.78 + \ln\left(\frac{D_{BH_4^-}^{1/2}}{k_s}\right) + \ln\left[\frac{(1-\alpha)\,n_a F\,\nu}{(RT)]^{1/2}}\right]\right\} \quad (7)$$

where E_p is the peak potential (V vs. SCE), E^0 is the formal potential of the electroactive $B(OH)_4^-/BH_4^-$ couple (−1.48 V vs. SCE), R is the universal gas constant (8.314 J K^{-1} mol^{-1}), T is the absolute temperature (K), α is the charge transfer coefficient for the oxidation step, n_a is the number of electrons involved in the rate determining step (being 1 the most likely value), F is the Faraday constant (96485 C mol^{-1}), $D_{BH_4^-}$ is the diffusion coefficient for BH_4^- (cm^2 s^{-1}), k_s is the standard heterogeneous rate constant for charge transfer (cm s^{-1}), and ν is the potential scan rate (V s^{-1}).

From the slope of the plots of E_p - ln ν (Fig. 3b) it is possible to calculate the α values for the BH_4^- oxidation process in the four tested electrode materials. In this way, values of α of 0.75, 0.76, 0.78, and 0.81 were obtained for the Pt, Pt–Ho, Pt–Sm, and Pt–Ce, respectively. These relatively high α values are typical of highly irreversible processes.

3.3. Chronopotentiometric measurements

By applying j values ranging from 5 to 100 mA cm^{-2}, chronopotentiometry (CP) curves with transition times, τ, ranging from 0.1 s to 15 s were obtained. Fig. 4a shows the potential–time curves obtained at j ranging from 13 to 60 mA cm^{-2}, at 25 °C, for the case of $NaBH_4$ oxidation on the single Pt electrode and Fig. 4b shows chronopotentiograms for the $NaBH_4$ oxidation in Pt and Pt–RE electrocatalysts, at 25 °C, and at a j value of 13 mA cm^{-2}.

Equivalent potential–time curves were obtained for the other solution temperatures. The curves were well reproducible, allowing precise measurement of the τ values, although the increase in the

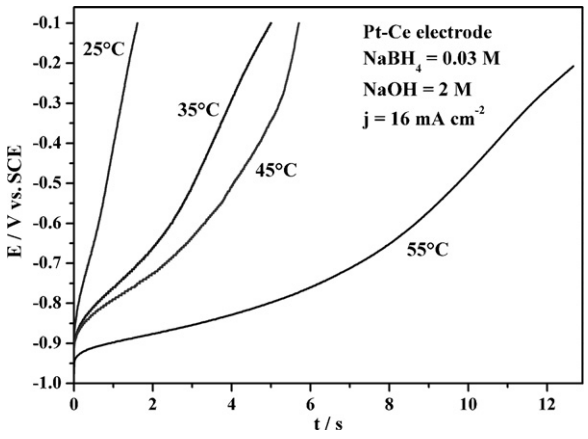

Fig. 5. Effect of temperature on potential–time curves for the oxidation of 0.03 M $NaBH_4$ in 2 M NaOH solution at a Pt–Ce electrode polarised at a j value of 16 mA cm^{-2}.

solution temperature slightly changes the shape of the CP curves by increasing the slope of the oxidation step.

In these potential–time curves, it is expected that for higher j, the extremely low values obtained for τ might be slightly distorted (increased) due to the double-layer charging effects which are more evident for these high j values. For very low j, the τ may be more enlarged than expected. This is due to the convective effects which start being important for longer experiment times, causing $j\tau^{1/2}$ to increase.

Fig. 5 shows potential–time curves for 0.03 M $NaBH_4$ at temperatures ranging from 25 to 55 °C, where the effect of temperature on the BH_4^- oxidation at a Pt–Ce alloy electrode is noticeable.

One can see that, for a given j, an increase in the cell temperature leads to an increase in τ. This effect is highlighted when working at lower j. At higher temperatures (>55 °C), the process is inevitably disturbed by convection effects generated by temperature gradients in solution, which complicates the analysis of the results.

Fig. 6 shows that the plots of $\tau^{1/2}$ vs. j^{-1} for the oxidation of 0.03 M $NaBH_4$ at the four tested electrode materials yield straight lines.

It is therefore permissible to apply the Sand equation (Eq. (8)) to determine the $n\,D_{BH_4^-}$ values from the slope of the $\tau^{1/2}$ vs. j^{-1} plots [67,71,81].

$$\tau^{1/2} = \frac{n F C_{BH_4^-}(\pi D_{BH_4^-})^{1/2}}{2j} \quad (8)$$

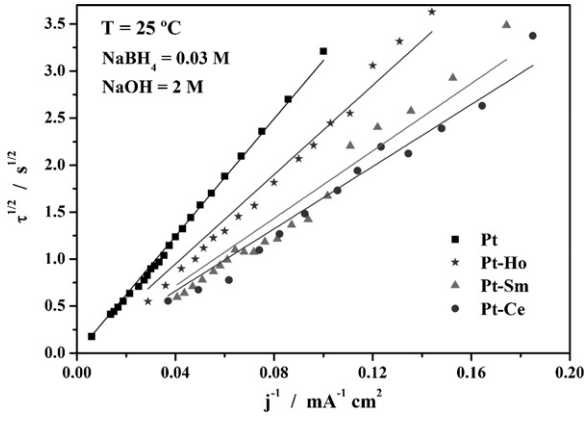

Fig. 6. Plots of $\tau^{1/2}$ vs. j^{-1} for the oxidation of 0.03 M $NaBH_4$ at the Pt and Pt–RE electrocatalysts, at 25 °C.

Table 1
Values of n for the BH_4^- oxidation peak, at various temperatures, for the four tested electrode materials.

	T (°C)			
	25	35	45	55
Pt	2.5	2.6	2.6	3.1
Pt–Ce	1.4	1.7	1.7	2.0
Pt–Sm	1.4	1.9	1.7	1.4
Pt–Ho	1.9	1.8	2.0	1.8

This expression was first derived by Sand in 1901 [81] and shows that because the concentration of the electroactive species, $C_{BH_4^-}$, is proportional to the square root of the transition time, $\tau^{1/2}$, CP can be used analytically.

Wang et al. [69] studied the BH_4^- oxidation in gold electrodes and developed an expression (Eq. (9)) that accounts for the temperature dependence of $D_{BH_4^-}$ in 2 M NaOH solutions, valid for temperatures ranging from 20 to 60 °C.

$$D_{BH_4^-} = 5.57 \times 10^{-3}\,\frac{\exp[-15.2 \times 10^3]}{(RT)} \quad (9)$$

An important aspect of the calculated $D_{BH_4^-}$ is that they are determined [69] without the need for known values of $C_{BH_4^-}$ and n, and hence Eq. (9) could be adopted for the present paper. However, very recent findings by Chatenet et al. [82] led to precise $D_{BH_4^-}$ values that are consistently higher by ca. 50% than most values presented in the literature in corresponding electrolyte solutions. Therefore, it is believed that the use of $D_{BH_4^-}$ values obtained by multiplying by a factor of two those calculated through Eq. (9), might not suffer from high inaccuracy. Accordingly, $D_{BH_4^-}$ values ranging from 2.42×10^{-5} to 4.24×10^{-5} $cm^2\,s^{-1}$ were calculated for the temperatures from 25 °C to 55 °C. Then, by application of the Sand equation (Eq. (8)) to the plots of $\tau^{1/2}$ vs. j^{-1} (see Fig. 6), the n values were obtained for the Pt and Pt–RE electrodes in the temperature range 25–55 °C (Table 1).

These deduced n values are, as expected, much inferior to the theoretical maximum number of electrons involved in the BH_4^- oxidation ($n = 8$). Values of n ranging from 2 to 4 are usually reported [30,35,41] for Pt and present results have also confirmed it. The Pt–RE alloys show lower n values indicating poor catalytic activity for the BH_4^- oxidation. In accordance to the Brewer-Engel theory [63], refined by Jaksic et al. [64–66], the alloying of Pt ($4f^{14}5d^96s^1$) with Ce ($4f^15d^16s^2$), or Sm ($4f^65d^06s^2$), or Ho ($4f^{11}5d^06s^2$), gives rise to composite d-transition metal catalysts with pronounced electrocatalytic activity towards the HER due to mutual combination of synergic activation of the (hyper-d-electronic) Pt element with hydride forming (hypo-d-electronic) elements. In such a context, the addition element Ce favours the BH_4^- heterogeneous hydrolysis, and the addition element Ho favours the BH_4^- direct oxidation. In other words, the Pt-RE alloys should favour the indirect oxidation of BH_4^-, which partially explains why their calculated n values are lower than those for the single Pt electrode. The slight dispersion in the obtained n values agrees with previous literature data [82]. Besides the already mentioned complexities in the system at given temperatures, such dispersion should be related to an intrinsic irreproducibility in the measurements, which render n calculations from the CP data less straightforward than theoretically expected.

Considering that the BH_4^- anodic oxidation can be assumed as a one-step irreversible process [37], the shape of the chronopotentiograms for the electrode reaction shown in Eq. (1) is described by Eq. (10) [67,80].

$$E = E^0 + \frac{RT}{(1-\alpha)F}\ln\frac{2k_s}{(\pi D_{BH_4^-})^{1/2}} + \frac{RT}{[(1-\alpha)F]\ln(\tau^{1/2} - t^{1/2})} \quad (10)$$

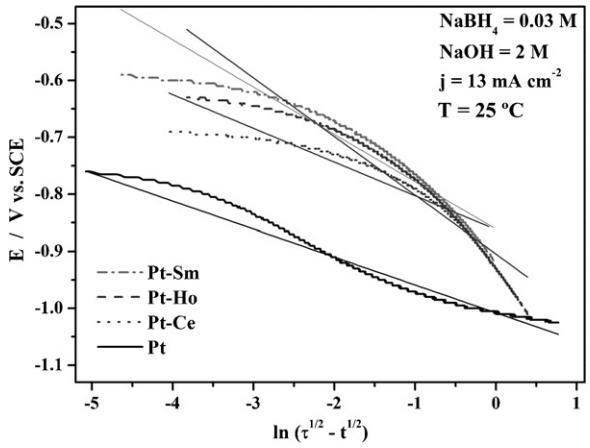

Fig. 7. Plots of E vs. $\ln(\tau^{1/2} - t^{1/2})$ at 25 °C for the oxidation of 0.03 M $NaBH_4$ in 2 M NaOH solution with the tested electrode materials, at a j value of 13 mA cm^{-2}.

To further elucidate the BH_4^- oxidation mechanism, semi-logarithmic plots were derived from the potential-time curves according to the representation of E vs. $\ln(\tau^{1/2} - t^{1/2})$ plots, as illustrated by the curves in Fig. 7.

According to Eq. (10), the intercepts of the linear fittings to the E vs. $\ln(\tau^{1/2} - t^{1/2})$ plots (Fig. 7) may be used to calculate the standard heterogeneous rate constants, k_s (cm s^{-1}), for the BH_4^- oxidation in the Pt and Pt–RE systems. Average k_s values of 2.6×10^{-7}, 1.2×10^{-7}, 2.2×10^{-6}, and 1.2×10^{-5} cm s^{-1} were obtained for the Pt, Pt–Ce, Pt–Sm, and Pt–Ho electrodes, respectively, indicating relatively higher oxidation kinetics for the Pt–Ho alloy and lower for the Pt–Ce alloy. Moreover, for each electrode material, the k_s values showed an expected [67,83] general increase with the solution temperature and minor changes with the applied j.

4. Conclusions

The electrooxidation of BH_4^- at Pt and at three Pt–RE binary alloys with equiatomic compositions has been studied by CV and CP, as a function of the working temperature. Anodic charge transfer coefficients, α, calculated by CV measurements, were very close for all the alloys and varied between 0.75 and 0.81. The number of exchanged electrons, n, found for the Pt–RE alloys was in the range 1.4–2.0 per BH_4^- anion, which is lower than that obtained experimentally for Pt ($2.5 < n < 3.1$) and that reported in the open literature leading to n between 2 and 4. Standard heterogeneous rate constants for charge transfer, k_s, ranging from 10^{-7} to 10^{-5} cm s^{-1}, were calculated for the Pt–RE alloys, with the Pt–Ho alloy showing the best oxidation kinetics and the Pt–Ce alloy the worst. Efforts are being made to correlate the microstructure of the Pt–RE alloys with their performance towards the BH_4^- oxidation reaction. The Brewer-Engel and Jaksic models were used to justify the obtained results. The lower n found for the studied alloys reduces the significance of the results, but there is a strong motivation to pursue the focus on the Pt–RE intermetallic alloys as good electrocatalysts for the BH_4^- oxidation, and at much lower cost than Pt alone. Accordingly, further studies are expected using other Pt–RE alloys, namely Pt–Dy, and at modified electrolyte compositions.

Acknowledgments

D.M.F. Santos thanks FCT, the Portuguese Foundation for Science and Technology for a postdoctoral research grant (SFRH/BPD/63226/2009).

References

[1] J.-H. Wee, J. Power Sources 155 (2006) 329.
[2] C. Cakanyildirim, M. Guru, Int. J. Hydrogen Energy 33 (2008) 4634.
[3] U.B. Demirci, P. Miele, Energy Environ. Sci. 2 (2009) 627.
[4] U.B. Demirci, O. Akdim, P. Miele, Int. J. Hydrogen Energy 34 (2009) 2638.
[5] B.H. Liu, Z.P. Li, J. Power Sources 187 (2009) 527.
[6] U.B. Demirci, O. Akdim, J. Andrieux, J. Hannauer, R. Chamoun, P. Miele, Fuel Cells 10 (2010) 335.
[7] C. Ponce de León, F.C. Walsh, D. Pletcher, D.J. Browning, J.B. Lakeman, J. Power Sources 155 (2006) 172.
[8] J.-H. Wee, J. Power Sources 161 (2006) 1.
[9] B.H. Liu, Z.P. Li, J. Power Sources 187 (2009) 291.
[10] J. Ma, N.A. Choudhury, Y. Sahai, Renew. Sust. Energy Rev. 14 (2010) 183.
[11] U.B. Demirci, J. Power Sources 172 (2007) 676.
[12] B.H. Liu, Z.P. Li, S. Suda, J. Power Sources 175 (2008) 226.
[13] C. Ponce de León, F.C. Walsh, A. Rose, J.B. Lakeman, D.J. Browning, R.W. Reeve, J. Power Sources 164 (2007) 441.
[14] Z.P. Li, B.H. Liu, J.K. Zhu, S. Suda, J. Power Sources 163 (2006) 555.
[15] K. Wang, J. Lu, L. Zhuang, J. Phys. Chem. C 111 (2007) 7456.
[16] F.A. Coowar, G. Vitins, G.O. Mepsted, S.C. Waring, J.A. Horsfall, J. Power Sources 175 (2008) 317.
[17] D.M.F. Santos, C.A.C. Sequeira, J. Electrochem. Soc. 157 (2010) B13.
[18] R. Jamard, J. Salomon, A. Martinent-Beaumont, C. Coutanceau, J. Power Sources 193 (2009) 779.
[19] N.A. Choudhury, R.K. Raman, S. Sampath, A.K. Shukla, J. Power Sources 143 (2005) 1.
[20] M.V. Mirkin, H. Yang, A.J. Bard, J. Electrochem. Soc. 139 (1992) 2212.
[21] B. Molina Concha, M. Chatenet, F. Maillard, E.A. Ticianelli, F.H.B. Lima, R.B. de Lima, Phys. Chem. Chem. Phys. 12 (2010) 11507.
[22] J.A. Gardiner, J.W. Collat, J. Am. Chem. Soc. 86 (1964) 3165.
[23] P. Krishnan, T.-H. Yang, S.G. Advani, A.K. Prasad, J. Power Sources 182 (2008) 106.
[24] L.C. Nagle, J.F. Rohan, J. Electrochem. Soc. 153 (2006) C773.
[25] M. Chatenet, M.B. Molina-Concha, J.-P. Diard, Electrochim. Acta 54 (2009) 1687.
[26] M. Chatenet, F.H.B. Lima, E.A. Ticianelli, J. Electrochem. Soc. 157 (2010) B697.
[27] H. Dong, R. Feng, X. Ai, Y. Cao, H. Yang, C. Cha, J. Phys. Chem. B 109 (2005) 10896.
[28] E.L. Gyenge, M.H. Atwan, D.O. Northwood, J. Electrochem. Soc. 153 (2006) A150.
[29] B.H. Liu, Z.P. Li, S. Suda, Electrochim. Acta 49 (2004) 3097.
[30] G. Rostamikia, M.J. Janik, Electrochim. Acta 55 (2010) 1175.
[31] J.A. Gardiner, J.W. Collat, J. Am. Chem. Soc. 87 (1965) 1692.
[32] J.A. Gardiner, J.W. Collat, Inorg. Chem. 4 (1965) 1208.
[33] Y. Okinaka, J. Electrochem. Soc. 120 (1973) 739.
[34] O.A. Sadik, H. Xu, A. Sargent, J. Electroanal. Chem. 583 (2005) 167.
[35] J.P. Elder, A. Hickling, Trans. Faraday Soc. 58 (1962) 1852.
[36] U.B. Demirci, F. Garin, Int. J. Green Energy 5 (2008) 148.
[37] E.L. Gyenge, Electrochim. Acta 49 (2004) 965.
[38] J.I. Martins, M.C. Nunes, R. Koch, L. Martins, M. Bazzaoui, Electrochim. Acta 52 (2007) 6443.
[39] D.A. Finkelstein, N. Da Mota, J.L. Cohen, H.D. Abruña, J. Phys. Chem. C 113 (2009) 19700.
[40] M.B. Molina-Concha, M. Chatenet, Electrochim. Acta 54 (2009) 6119.
[41] M. Simões, S. Baranton, C. Coutanceau, J. Phys. Chem. C 113 (2009) 13369.
[42] M. Simões, S. Baranton, C. Coutanceau, Electrochim. Acta 56 (2010) 580.
[43] Y. Chen, X. Wang, L. Chen, C.P. Chen, Q. Wang, C.A.C. Sequeira, J. Alloys Compd. 421 (2006) 223.
[44] Y. Chen, C.A.C. Sequeira, X. Song, R. Neto, Q. Wang, Int. J. Hydrogen Energy 27 (2002) 63.
[45] Y. Chen, C.A.C. Sequeira, T. Allen, C.P. Chen, J. Alloys Compd. 404–406 (2005) 661.
[46] Y. Chen, C.A.C. Sequeira, X. Song, C.P. Chen, Z. Phys. Chem. 220 (2006) 631.
[47] F. Rosalbino, D. Macciò, E. Angelini, A. Saccone, S. Delfino, Int. J. Hydrogen Energy 33 (2008) 2660.
[48] F. Rosalbino, D. Macciò, E. Angelini, A. Saccone, S. Delfino, J. Alloys Compd. 403 (2005) 275.
[49] C.A.C. Sequeira, D.M.F. Santos, P.S.D. Brito, Energy 36 (2011) 847.
[50] D. Macciò, F. Rosalbino, A. Saccone, S. Delfino, J. Alloys Compd. 391 (2005) 60.
[51] A.O. Neto, A.Y. Watanabe, M. Brandalise, M.M. Tusi, R.M. de, S. Rodrigues, M. Linardi, E.V. Spinacé, C.A.L.G.O. Forbicini, J. Alloys Compd. 476 (2009) 288.
[52] A.O. Neto, A.Y. Watanabe, R.M. de, S. Rodrigues, M. Linardi, C.A.L.G.O. Forbicini, E.V. Spinacé, Ionics 14 (2008) 577.
[53] K.W. Lux, E.J. Cairns, J. Electrochem. Soc. 153 (2006) A1132.
[54] K.W. Lux, E.J. Cairns, J. Electrochem. Soc. 153 (2006) A1139.
[55] M. Sauer, S. Raetz, V. Ohm, M. Merkens, C. Sauer, D. Schmitz, H. Schilder, H. Lueken, J. Alloys Compd. 246 (1997) 147.
[56] T. Wang, F. Li, J. Li, J. Alloys Compd. 207–208 (1994) 393.
[57] I.H. Son, J. Power Sources 159 (2006) 1266.
[58] C.A.C. Sequeira, High temperature oxidation, in: R. Winston Revie (Ed.), Uhlig's Corrosion Handbook, 3rd ed., The Electrochemical Society Series, Wiley, Hoboken, NJ, 2011, ISBN: 978-0-470-08032-0.
[59] C.M.Y. Yeung, S.C. Tsang, J. Mol. Catal. A 322 (2010) 17.
[60] U.B. Demirci, P. Miele, C. R. Chim. 12 (2009) 943.
[61] L. Vračar, B.E. Conway, J. Electroanal. Chem. 277 (1990) 253.
[62] L. Vračar, B.E. Conway, Int. J. Hydrogen Energy 15 (1990) 701.
[63] M.M. Jaksic, Electrochim. Acta 29 (1984) 1539.
[64] M.M. Jaksic, Int. J. Hydrogen Energy 12 (1987) 727.

[65] M.M. Jaksic, Int. J. Hydrogen Energy 11 (1986) 519.
[66] S.G. Neophytides, S. Zafeiratos, G.D. Papakonstantinou, J.M. Jaksic, F.E. Paloukis, M.M. Jaksic, Int. J. Hydrogen Energy 30 (2005) 131.
[67] D.M.F. Santos, C.A.C. Sequeira, J. Electrochem. Soc. 157 (2010) F16.
[68] D.M.F. Santos, C.A.C. Sequeira, Electrochim. Acta 55 (2010) 6775.
[69] K. Wang, J. Lu, L. Zhuang, J. Electroanal. Chem. 585 (2005) 191.
[70] M.H. Atwan, D.O. Northwood, E.L. Gyenge, Int. J. Hydrogen Energy 32 (2007) 3116.
[71] M. Chatenet, F. Micoud, I. Roche, E. Chainet, Electrochim. Acta 51 (2006) 5459.
[72] E. Sanli, B. Uysal, M.L. Aksu, Int. J. Hydrogen Energy 33 (2008) 2097.
[73] E. Sanli, H. Celikkan, B. Uysal, M.L. Aksu, Int. J. Hydrogen Energy 31 (2006) 1920.
[74] G. Parrour, M. Chatenet, J.-P. Diard, Electrochim. Acta 55 (2010) 9113.
[75] S. Colominas, J. McLafferty, D.D. Macdonald, Electrochim. Acta 54 (2009) 3575.
[76] H. Celikkan, M. Sahin, M.L. Aksu, T. Nejat Veziroglu, Int. J. Hydrogen Energy 32 (2007) 588.
[77] M.H. Atwan, C.L.B. Macdonald, D.O. Northwood, E.L. Gyenge, J. Power Sources 158 (2006) 36.
[78] P. He, Y. Wang, X. Wang, F. Pei, H. Wang, L. Liu, L. Yi, J. Power Sources 196 (2011) 1042.
[79] S. Trasatti, O.A. Petrii, J. Electroanal. Chem. 327 (1992) 353.
[80] A.J. Bard, L.R. Faulkner, Electrochemical Methods: Fundamentals and Applications, 2nd ed., John Wiley & Sons, NY, 2001.
[81] H.J.S. Sand, Philos. Mag 1 (1901) 45.
[82] M. Chatenet, M.B. Molina-Concha, N. El-Kissi, G. Parrour, J.-P. Diard, Electrochim. Acta 54 (2009) 4426.
[83] D.M.F. Santos, C.A.C. Sequeira, J. Electrochem. Soc. 156 (2009) F67.